PS Geological Controls on Formation Water Salinity Distribution Southeastern Greater Natural Buttes Field, Uinta Basin, Utah*

Tuba Evsan[1], Matthew J. Pranter[2], and Marc Connolly[3]

Search and Discovery Article #20213 (2013)**
Posted October 21, 2013

*Adapted from a poster presentation given at AAPG Rocky Mountain Section Meeting, Salt Lake City, Utah, September 22-24, 2013

[1]Department of Geological Sciences, University of Colorado, Boulder, Colorado (Tuba.Evsan@colorado.edu)
[2]ConocoPhillips School of Geology and Geophysics, University of Oklahoma, Norman, Oklahoma
[3]PetroLith, LLC, Littleton, Colorado

Abstract

Tight-gas sandstone reservoirs of the Upper Cretaceous Mesaverde Group in the Greater Natural Buttes (GNB) Field have variable fluid saturations along with low matrix porosity and permeability. In order to build more reliable saturation models, it is significant to determine resistivity of formation water, which is one of the input parameters in water saturation calculations. This study mainly investigates how formation water resistivity and salinity vary stratigraphically and spatially. For petrophysical analysis, the study interval was divided into seven stratigraphic zones based on net-to-gross ratio and variation in resistivity. Formation water resistivity derived from Pickett-plot analysis was used with formation temperature to determine formation water salinity distribution per zone. Temperature data from production logs show that the Wasatch Formation and Mesaverde Group have higher geothermal gradients than formations that are stratigraphically above. Therefore, formation temperature was estimated using these gradients, which are consistent through the study interval. Petrophysical analysis indicates more fresh water is present in the western part of the study area coinciding with the trace of a basement fault. Salinity decreases stratigraphically downward while water saturation is variable within the study interval. Average formation water resistivity per zone ranges between 0.048 ohm-m to 0.064 ohm-m based on Pickett-plot analysis, while average formation water salinity per zone ranges between 55,000 ppm to 86,000 ppm. Furthermore, the average effective bulk-volume water is nearly constant around 3.5% suggesting that as being a basin-centered gas accumulation, most sandstones within the study interval are close to irreducible water saturation. A combination of different geological mechanisms might account for observed salinity variations. The increase in freshness stratigraphically downward may be due to basement faulting and associated natural fracture system enhancing upward movement of fresher formation water. In addition, coal and sediment dewatering in stratigraphic units below study interval might be the source of fresher formation water in this potentially closed hydrological system, whereas distinct horizontal layering and continuity of different petrophysical rock types might result in observed salinity trends in the area.

Geological controls on formation water salinity distribution
southeastern Greater Natural Buttes Field, Uinta Basin, Utah

Tuba Evsan[1], Matthew J. Pranter[2], Marc Connolly[3]

[1] Department of Geological Sciences, University of Colorado, Boulder, Colorado
[2] ConocoPhillips School of Geology and Geophysics, University of Oklahoma, Norman, Oklahoma
[3] PetroLith, LLC, Littleton, Colorado

University of Colorado at Boulder

Reservoir Characterization and Modeling Laboratory

Abstract

Tight-gas sandstone reservoirs of the Upper Cretaceous Mesaverde Group in the Greater Natural Buttes (GNB) Field have variable fluid saturations along with low matrix porosity and permeability. In order to build more reliable saturation models, it is significant to determine resistivity of formation water which is one of the input parameters in water saturation calculations. This study mainly investigates how formation water resistivity and salinity vary stratigraphically and spatially.

For petrophysical analysis, the study interval was divided into seven stratigraphic zones based on net-to-gross ratio and variation in resistivity. Formation water resistivity derived from Pickett-plot analysis was used with formation temperature to determine formation water salinity distribution per zone. Temperature data from production logs show that the Wasatch Formation and Mesaverde Group have higher geothermal gradients than formations that are stratigraphically above. Therefore, formation temperature was estimated using these gradients which are consistent through the study interval. Petrophysical analysis indicates more fresh water is present in the western part of the study area coinciding with the trace of a basement fault. Salinity decreases stratigraphically downward while water saturation is variable within the study interval. Average formation water resistivity per zone ranges between 0.048 ohm-m to 0.064 ohm-m based on Pickett-plot analysis, while average formation water salinity per zone ranges between 55,000 ppm to 86,000 ppm. Furthermore, the average effective bulk-volume water is nearly constant around 3.5% suggesting that as being a basin-centered gas accumulation, most sandstones within the study interval are close to irreducible water saturation.

A combination of different geological mechanisms might account for observed salinity variations. The increase in freshness stratigraphically downward may be due to basement faulting and associated natural fracture system enhancing upward movement of fresher formation water. In addition, coal and sediment dewatering in stratigraphic units below study interval might be the source of fresher formation water in this potentially closed hydrological system, whereas distinct horizontal layering and continuity of different petrophysical rock types might result in observed salinity trends in the area.

Research Objectives

Because determining formation water resistivity and salinity variations is important in building more reliable saturation models, this study addresses the following questions as related to the study area in the GNB Field: 1) How does formation water salinity vary stratigraphically and spatially? 2) What combination of mechanisms (i.e. fractures, imbibition) results in variation of formation water salinity? 3) Does the spatial distribution of the highest reservoir quality rock type relate to the salinity distribution? The results of this study provide a better understanding of the log-derived methodology to determine formation water resistivity that is applicable in the analysis of many tight-gas sandstones. Therefore, the methods presented in this study can also be applied to analogous tight-gas sandstone formations.

Study Area

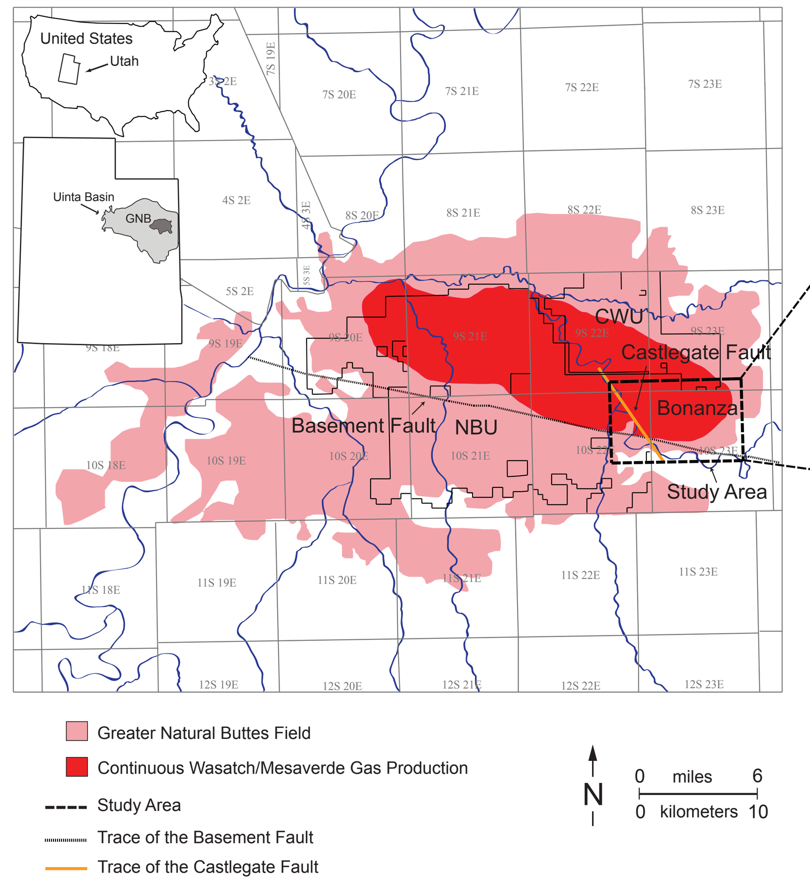

Map of the Greater Natural Buttes (GNB) Field including the location of Fairway which is the area of continuous Wasatch/ Mesaverde gas production. The approximate boundaries of the Natural Buttes Unit (NBU), Chapita Wells Unit (CWU), and Bonanza Field (Bonanza) are shown with a solid black line. Modified from Stancel et al. (2008).

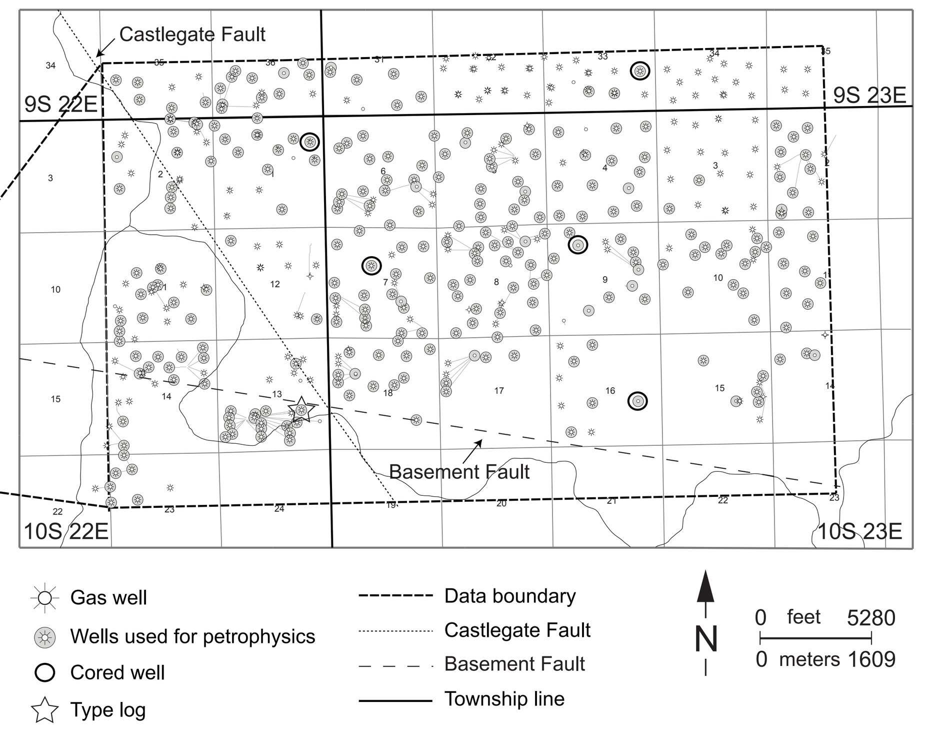

Detailed study area. The basement fault shown offsets below the bottom of the Mancos Shale and lower horizons, while it does not offset the non-marine portion of the Mesaverde (e.g. the study interval) and it is expressed as a subtle noise in the non-marine portion. There are faults in the shallower interval in the GNB Field along the trend of this deeper seated fault. The Castlegate Fault coincides with the trace of the White River, while it was only hypothesized because of the very poor seismic data due to presence of a valley. Although there is reasonable seismic evidence of the basement fault, the Castlegate Fault is speculative (Butler, pers.comm., 2013).

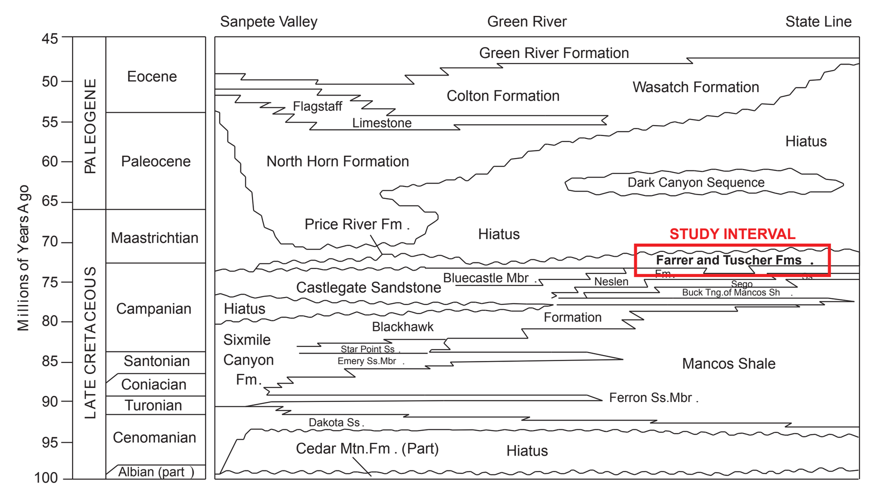

Chronostratigraphic chart showing the stratigraphic nomenclature for the eastern Utah. The study focuses on Farrer and Tuscher Formations of the Upper Cretaceous Mesaverde Group. Modified from Franczyk et al. (1990).

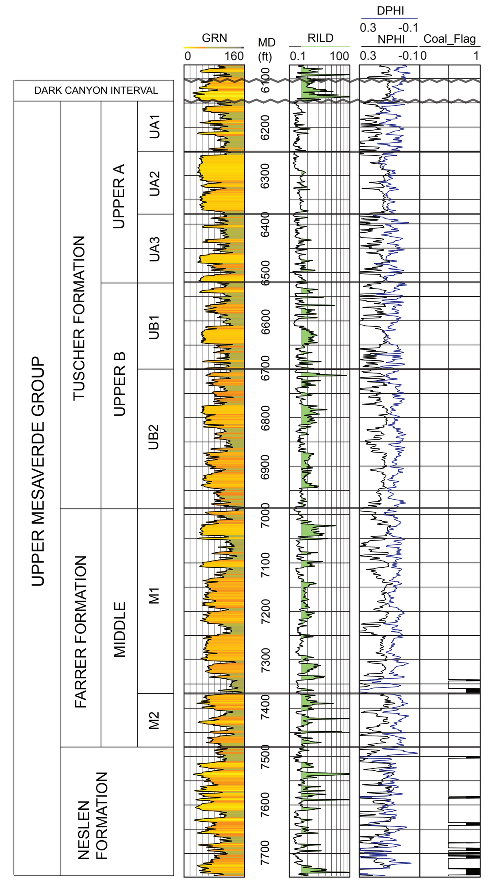

Type log for the study area (see basemap for the location). The resistivity values higher than 20 ohm-m are color coded green in order to separate sandstone from shale. Dark Canyon interval is a part of the Wasatch Formation.

Conceptual Petrophysical Model

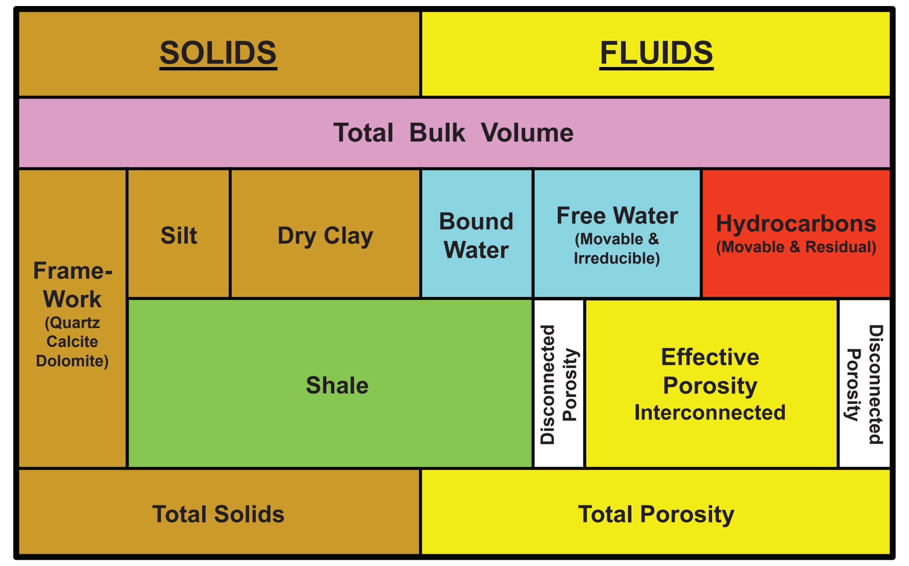

Bulk volume chart representing conceptual petrophysical model (Courtesy of Marc Connolly). Total rock volume consists of total solids (shale and non-shale volume) and fluids. One of the main practices in petrophysical workflow is to find the shale volume and bound-water associated with clays that help to further calculate effective porosity, free-water saturation and hydrocarbon volume.

Log Normalization

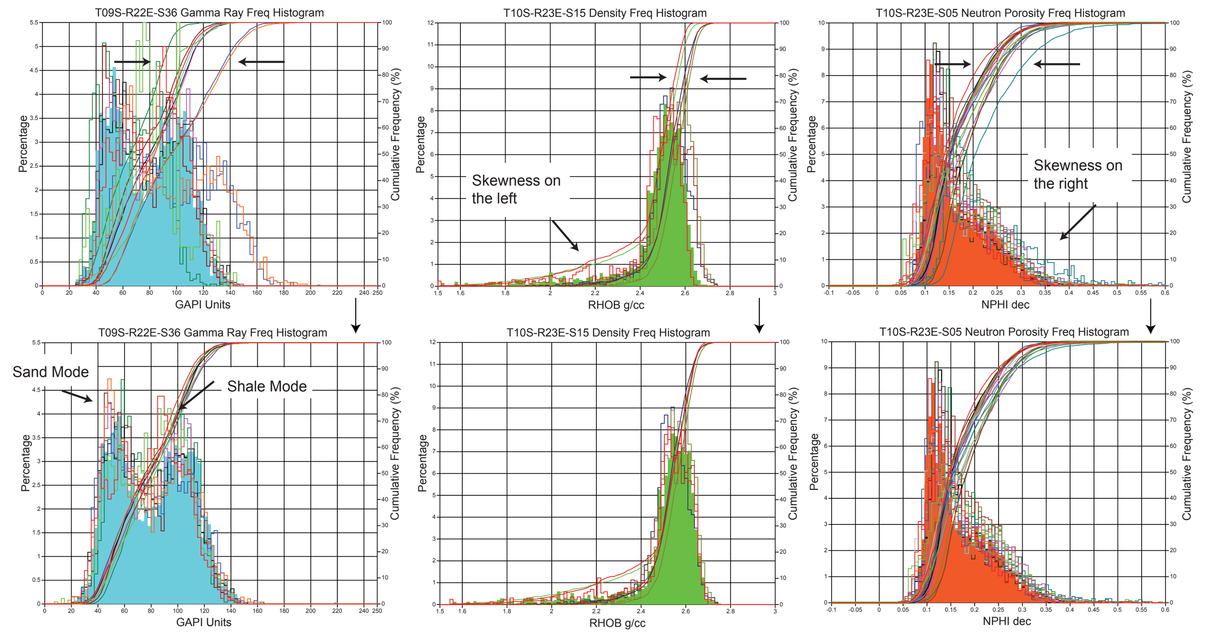

Composite histograms (before and after normalization) for the gamma-ray, density, and neutron-porosity logs. Gamma-ray histogram shows bimodal distribution, whereas skewness can be seen both in neutron porosity and density logs which is caused by the presence of shale. Sand and shale modes in the gamma-ray histogram, and skewness in bulk-density and neutron-porosity logs are also displayed in the figure.

Pickett-plot Analysis

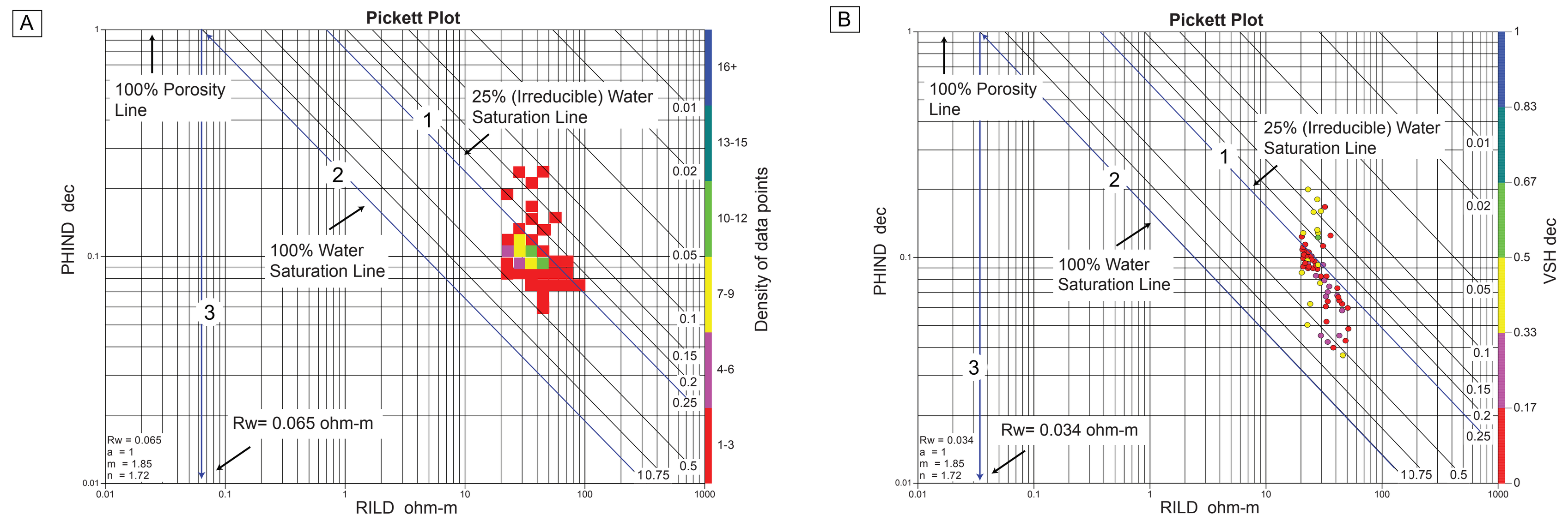

Pickett Plot examples from two different wells for the zones UB1 and UA2. Both the density of data points (A) and the approximate linearity in the upper bound of the data (B) were used to position the irreducible water saturation line (Swirr=25%). After adjusting Swirr line on the graph (1), 100% water saturated line is extended to the 100% porosity line (2) to determine formation water resistivity (Rw, [3]). The distance between water saturation lines is determined by the saturation exponent "n", and the slope of the water saturation lines is determined by the cementation exponent "m". Exponents "m" and "n" were set at 1.85 and 1.72 in Pickett-plots based on a Mesaverde study in Piceance Basin (Merkel, 2006).

Temperature Data

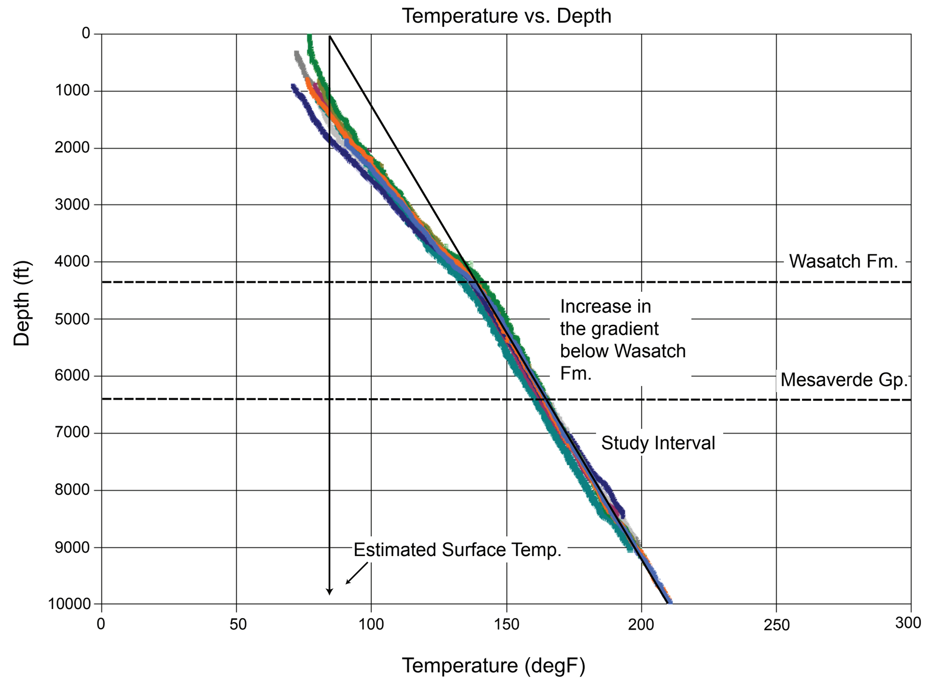

Temperature curves recorded by the CBL tool for several wells in the study area (colored lines). Approximate depths of Wasatch Formation and Mesaverde Group are shown by black dashed lines. To maintain a linear gradient, slope for the Mesaverde portion of each curve was extrapolated to the surface to estimate a surface temperature (solid black lines). Temperature data forthe other wells in the area were obtained by linearizing the average estimated surface temperature using the average slope (Miller, pers. comm., 2013).

Formation Water Salinity Distribution

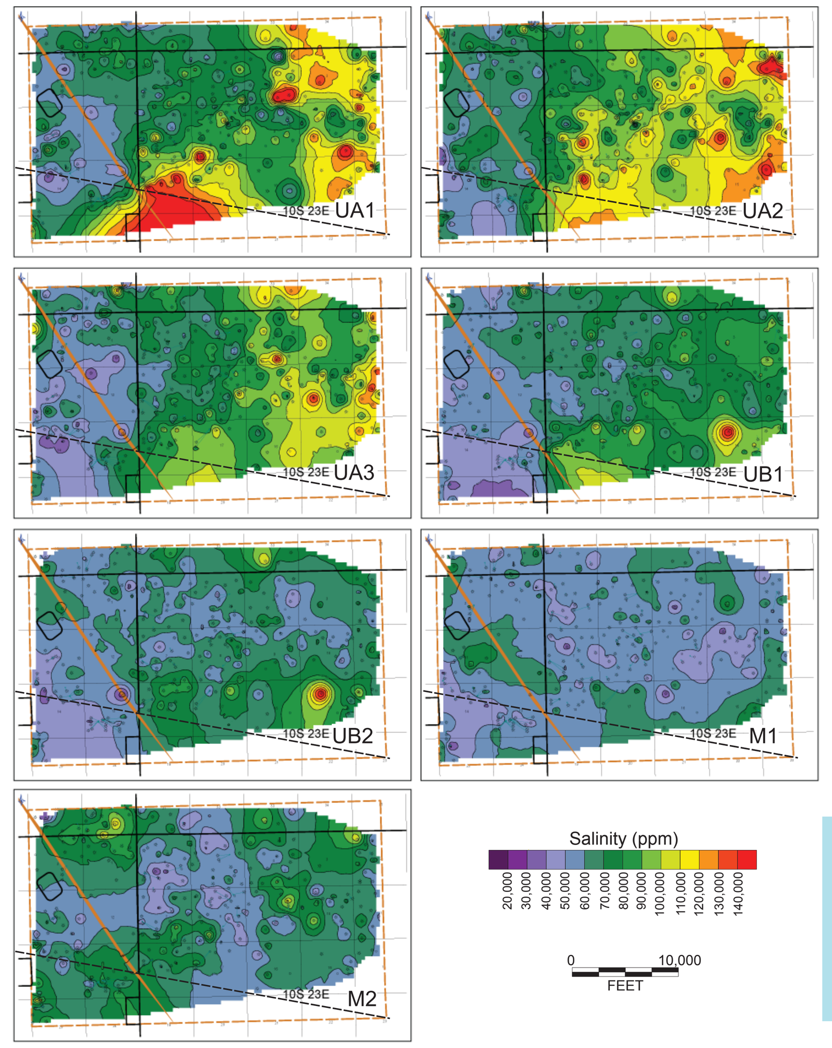

Maps of average formation water salinity distribution per zone (from top [UA1] to bottom [M2]). Northwest-trending line on the maps is the Castlegate Fault and the black dashed line is the basement fault. The trend shows the presence of fresher water on the west, and it also coincides with the trace of faults. Salinity decreases stratigraphically downward.

Zone	N	Max.	Min.	Mean	Median	Mode	Std. Dev.	CV (%)
UA1	267	184,800	28,600	82,210	78,000	57,100	27,470	33.41
UA2	267	170,700	34,300	86,350	85,400	85,400	26,690	30.91
UA3	268	147,400	24,900	75,780	71,650	68,400	23,720	31.29
UB1	257	150,100	31,600	66,930	63,200	59,400	17,250	25.77
UB2	248	149,000	23,200	61,833	62,200	52,100	14,000	22.65
M1	243	86,300	27,600	55,200	54,600	52,400	9,690	17.55
M2	242	122,400	31,900	64,190	62,750	65,700	16,780	26.14

Salinity (ppm) statistics per zone. The average salinity for the entire interval ranges between 55,200 ppm to 86,350 ppm showing the highest dispersion for the zone UA1 (CV=33.41%) and lowest dispersion for the zone M1 (CV=17.55%). CV: Coefficient of variance.

VSH and VCL Calculations

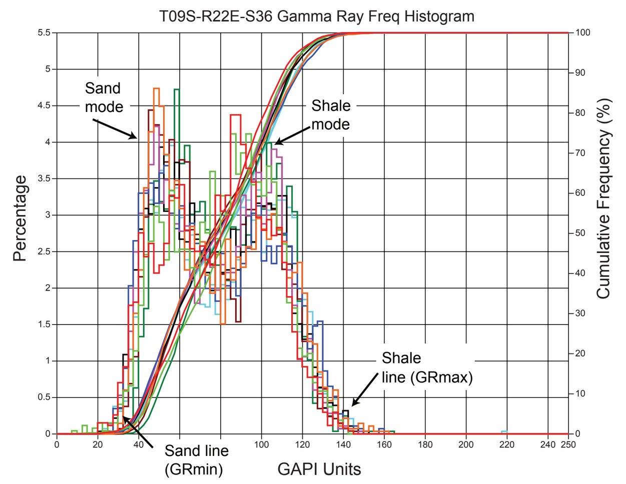

Figure shows the gamma-ray frequency histogram. Histograms were prepared for each section in the study area. GRmin and GRmax values were determined for each section separately by selecting inflection points on the left and right shoulders of the histogram.

Neutron-density cross-plot technique to find clay volume (VCL, %). In order to determine sandstone points, multi-well cross-plot was generated without filtering shale. Sandstone points on the graph were determined as [0.2.5 g/cc] and [0.15, 2.25 g/cc] for the neutron-porosity and density log respectively in order to capture the majority of the data on the plot.

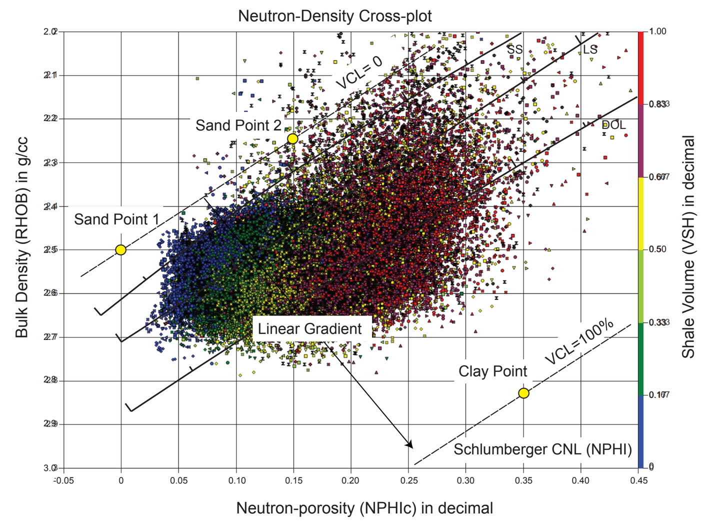

Irreducible Water Saturation

Buckles plot example. For the study interval, usually the points lie on the plot are not positioned along the same iso-BVW line and clear hyperbolic trend is not observed in the graphs (e.g. due to shalines). In this example, bulk-volume water irreducible (BVWirr) is determined as 0.014 (1.4%) for the zone UA2.

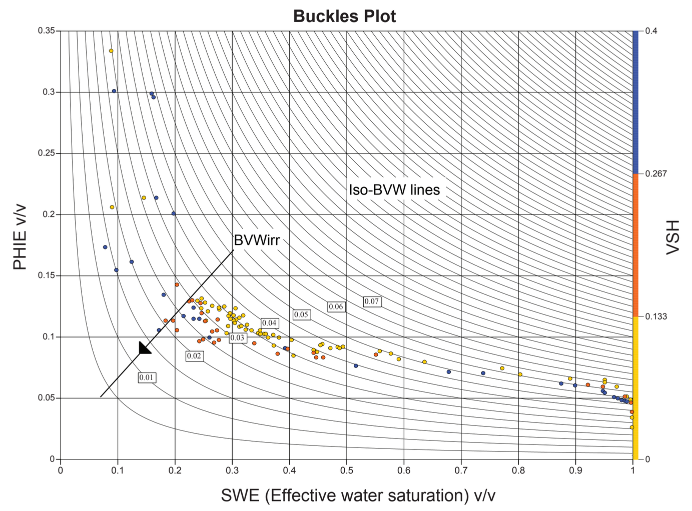

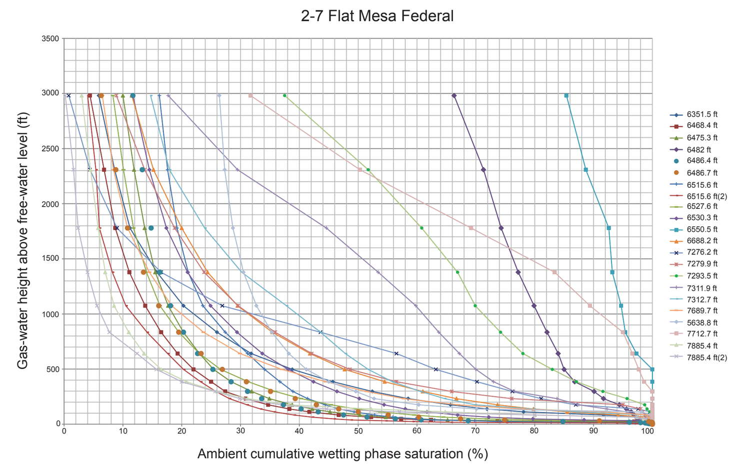

The graph shows data for the well 2-7 Flat Mesa Federal. The data were provided by Byrnes and Cluff (2009) and include gas-brine capillary pressure data for 21 samples. The curves usually present asymptotic irreducible water saturations (Swirr) around 10% to 30% which are usually higher than the log derived (Buckles plot) Swirr.

Bulk-volume Water Distribution

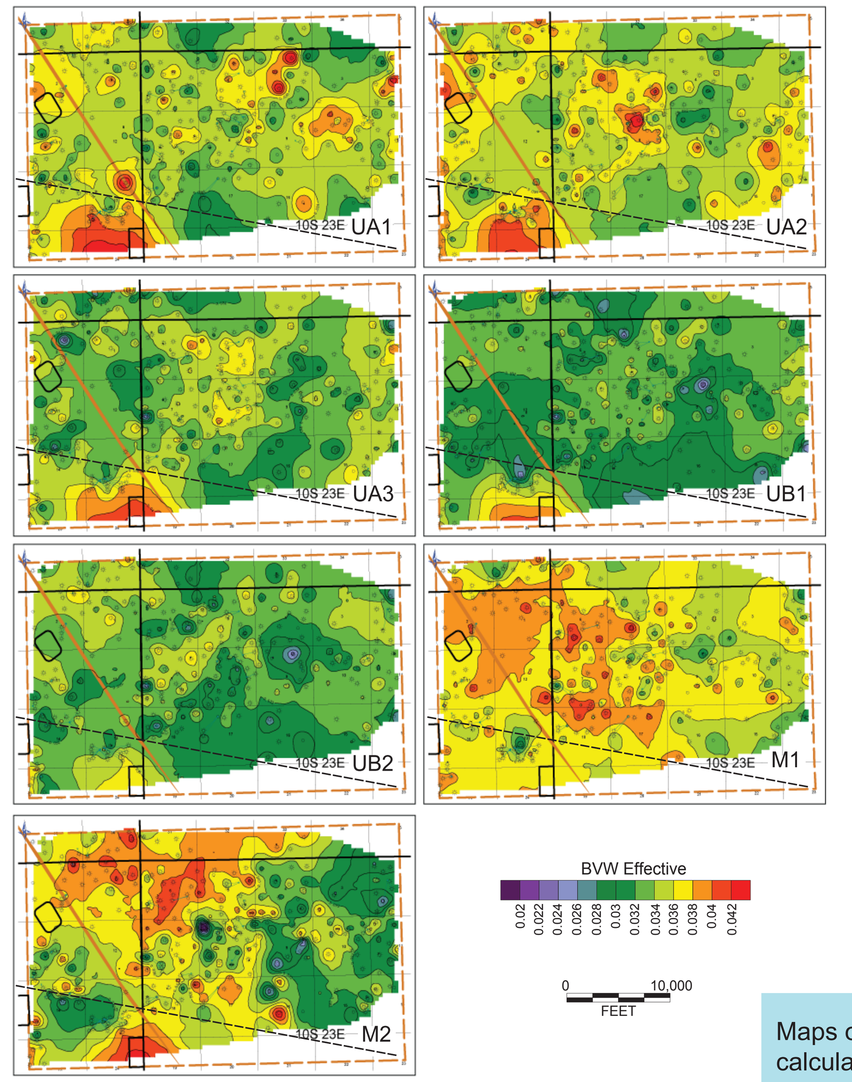

Archie Equation	Waxman-Smits Equation
a = 1.00	a = 1.00
m = 1.85	m = 1.85
n = 1.72	n = 1.72
Porosity: Effective porosity (PHIE)	Porosity: Total porosity (PHIND)
Resistivity: True formation resistivity	Resistivity: True formation resistivity
Rw: Obtained from Pickett Plots	Rw: Obtained from Pickett Plots
Temperature: Linearized surface temperature	Temperature: Linearized surface temperature
	PhitSh: Total porosity of shale (taken as 0.035)
	VCL: Volume of clay (from GR log and NDXP)
	CEC ≅ 3.7360*VSH + 1.1375(VSH^2)

Input parameters used for Archie and Waxman-Smits equations. The exponents "m" and "n" were taken from the Mesaverde study in the Piceance Basin (Merkel, 2006). CEC was calculated using the gamma ray index (VSH) (Chisholm et al., 1987) and VSH was set to 0.0001 for shale-free zones before calculating CEC. Total porosity of shale comes from the average humidity dried Boyles Law helium core porosity of the Mesaverde Group fluvial shale (Kukal and Hill, 1986). NDXP: Neutron-density cross-plot.

Maps of average effective bulk-volume water (dec) per zone calculated using Waxman-Smits equation. Largest values are in zones M1 and M2. No distinct pattern is observed except for a north-east trend in UA3, UB2, and M2. Zones M1 and M2 have higher bulk-volume water relative to the upper zones.

Petrophysical Rock Type Classification

	Examples
RX1	Structureless sandstone Cross-bedded sandstone
RX2	Planar-laminated sandstone
RX3	Ripple cross-bedded sandstone Mottled sandstone
RX4	Mudstone
RX5	Mudstone Claystone Coal (rarely)

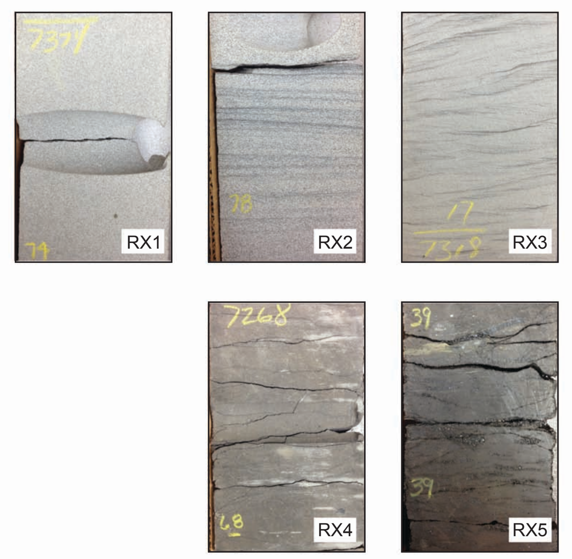

Examples of petrophysical rock types based on core-to-log comparisons and core descriptions. Rock Type 1 (RX1), Rock Type 2 (RX2), and Rock Type 3 (RX3) are usually sandstone facies and they are considered as potential reservoir rocks. The difference between them is based on change in sedimentary structure and grain size. RX1: Highest reservoir quality rock type.

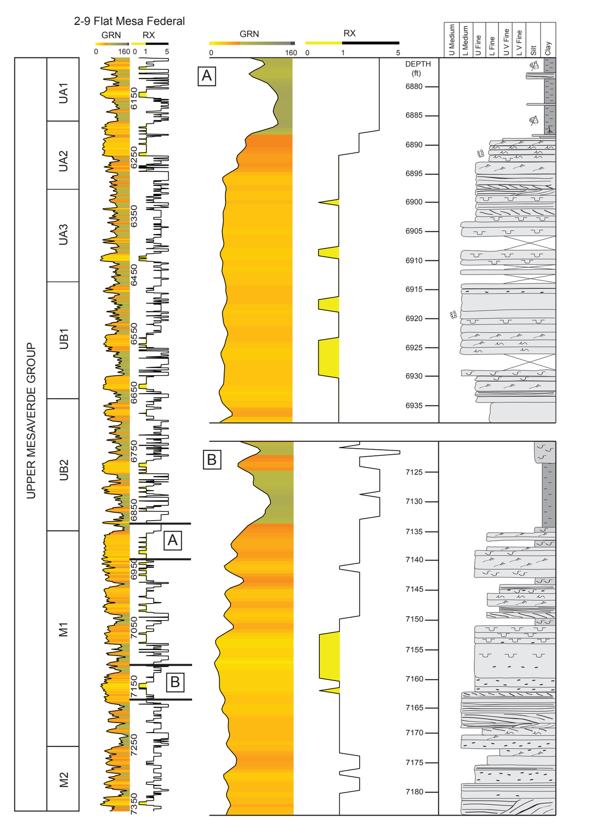

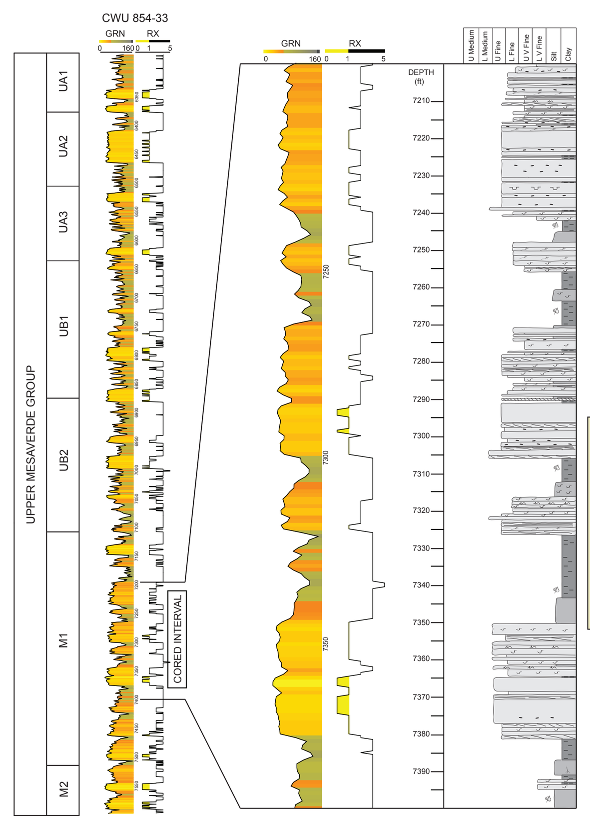

No Name Canyon Federal and CWU 854-33 cores; core descriptions compared to gamma-ray log and petrophysical rock type curve signatures.

Rock Type Model

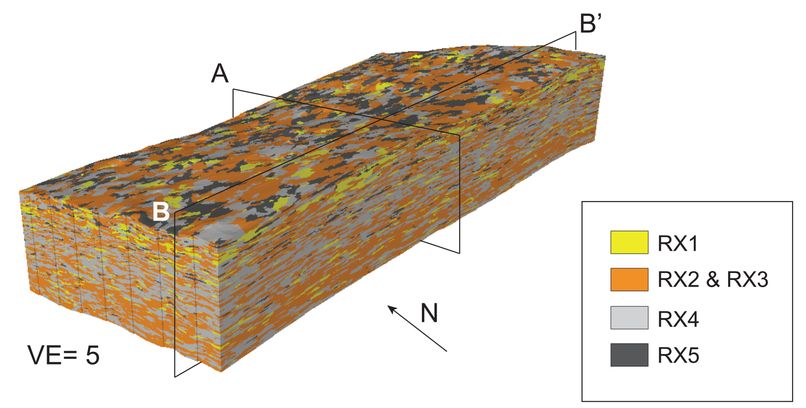

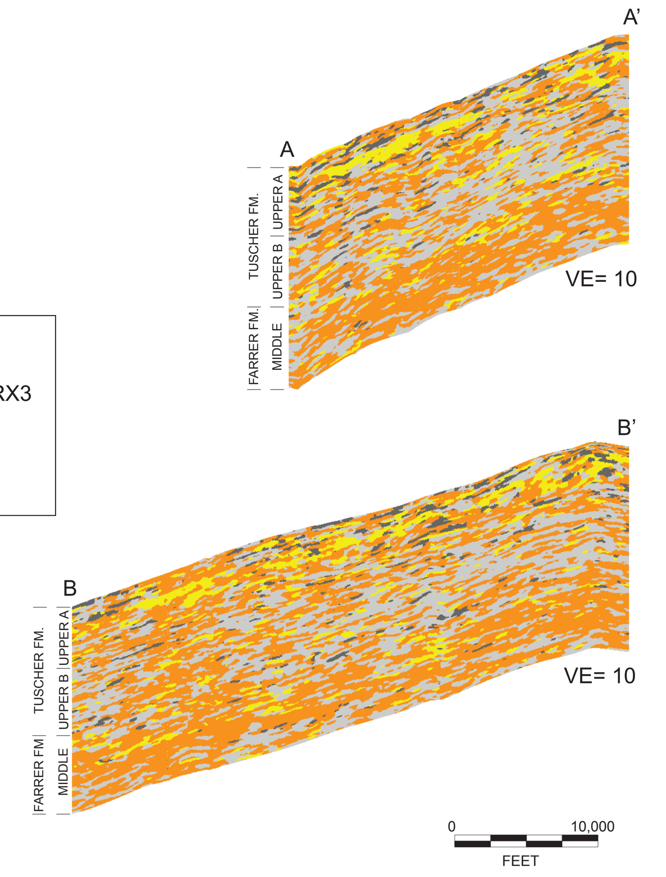

Three-dimensional petrophysical rock type model using Sequential Indicator Simulation (SIS). Because there is not a sharp distinction in petrophysical characteristics between Rock Type 2 (RX2) and Rock Type 3 (RX3) compared to Rock Type 1 (RX1), RX2 and RX3 were grouped together in the rock type model.

Vertical Salinity Profile

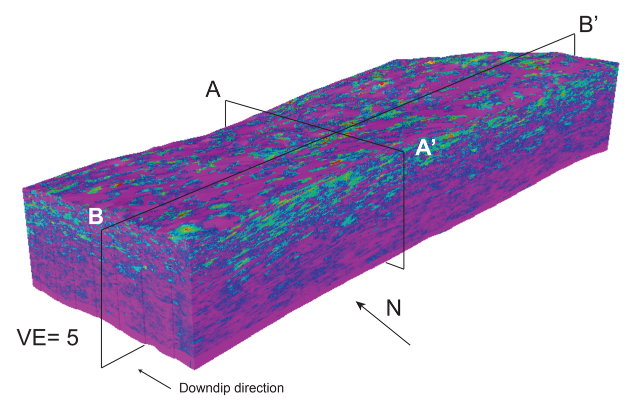

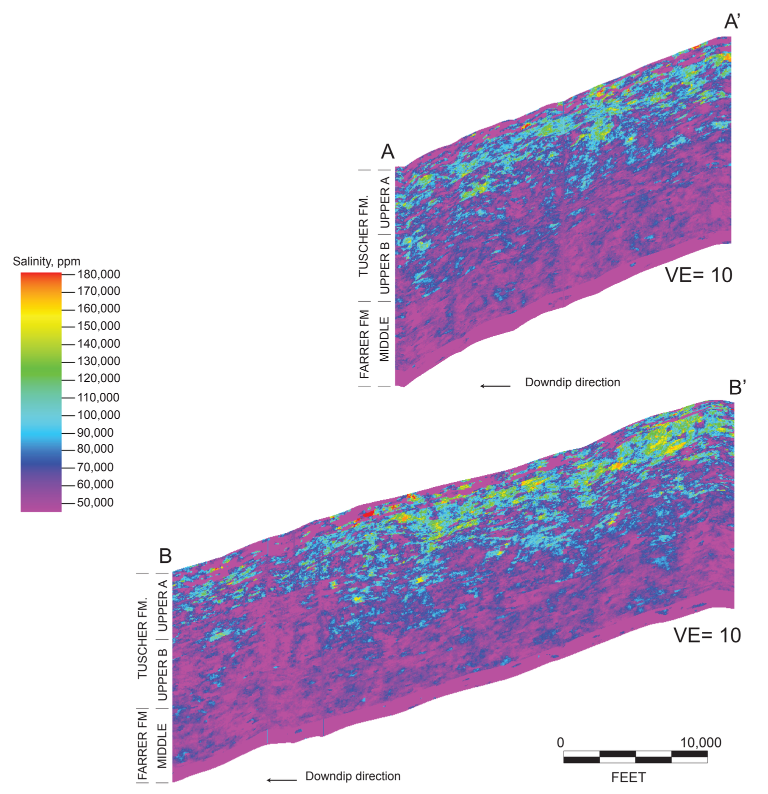

Formation water salinity distribution that were modeled using Sequential Gaussian Simulation (SGS). Petrophysical rock type model was used as a constraint when the salinity model was generated.

Controls on Salinity Distribution

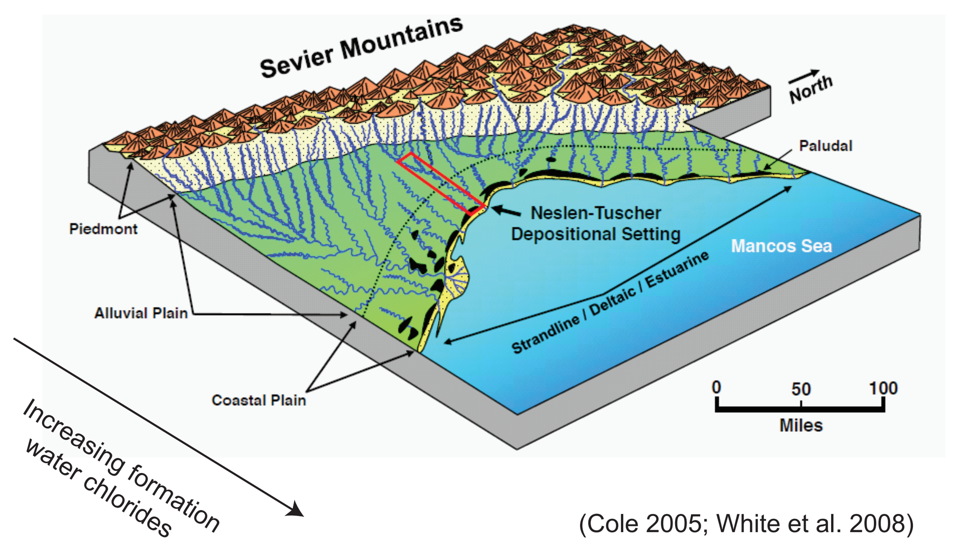

(Cole 2005; White et al. 2008)

Conclusions

Pickett-plot analysis was used to determine formation water resistivity and salinity variations in the area.

Formation water salinity ranges between 55,200 ppm to 86,350 ppm for the entire interval, while it decreases stratigraphically downward.

Relatively higher effective bulk-volume percentages for the Farrer Formation might also indicate the upward movement of fresher water from stratigraphically lower units.

An integration of multiple mechanisms; basement faulting and/or associated fracture network, coal and sediment dewatering, and spatial rock distribution are considered primary controls on observed formation water salinity distribution considering a more closed hydrological system.

Acknowledgements

Anadarko Petroleum Corporation
Chevron
ExxonMobil
OXY
QEP Resources, Inc.
Suncor Energy
WPX Energy
iReservoir.com
Schlumberger
IHS
JASON A CGG Company